

Long non-coding RNA FEZF1-AS1 facilitates non-small cell lung cancer progression via the ITGA11/miR-516b-5p axis

HENG SONG¹, HUI LI¹, XIAOSONG DING¹, MINGLEI LI¹, HAITAO SHEN^{1,2},
YUEHONG LI³, XIANGHONG ZHANG^{1,3} and LINGXIAO XING^{1,2}

¹Department of Pathology; ²Center of Metabolic Diseases and Cancer Research, Institute of Medical and Health Science, Hebei Medical University, Shijiazhuang, Hebei 050017; ³Department of Pathology, Second Hospital of Hebei Medical University, Shijiazhuang, Hebei 050000, P.R. China

Received May 6, 2020; Accepted September 8, 2020

DOI: 10.3892/ijo.2020.5142

Abstract. Long non-coding RNAs (lncRNAs) have emerged as key players in the development and progression of cancer. FEZ family zinc finger 1 antisense RNA 1 (FEZF1-AS1) is a novel lncRNA that is involved in the development of cancer and acts as a potential biomarker for cancer. However, the clinical significance and molecular mechanism of FEZF1-AS1 in non-small cell lung cancer (NSCLC) remains uncertain. In the present study, FEZF1-AS1 was selected using Arraystar Human lncRNA microarray and was identified to be upregulated in NSCLC tissues and negatively associated with the overall survival of patients with NSCLC. Loss-of-function assays revealed that FEZF1-AS1 inhibition decreased cell proliferation and migration, and arrested cells at the G₂/M cell cycle phase. Mechanistically, FEZF1-AS1 expression was influenced by N⁶-methyladenosine (m⁶A) modification. Since FEZF1-AS1 was mainly located in the cytoplasmic fraction of NSCLC cells, it was hypothesized that it may be involved in competing endogenous RNA regulatory network to impact the prognosis of NSCLC. Via integrating Arraystar Human mRNA microarray data and miRNA bioinformatics analysis, it was revealed that ITGA11 expression was decreased with loss of FEZF1-AS1 and increased with gain of FEZF1-AS1 expression, and microRNA (miR)-516b-5p inhibited the expression levels of both FEZF1-AS and ITGA11. RNA-binding protein immunoprecipitation and RNA pulldown assays further demonstrated that FEZF1-AS1 could bind to miR-516b-5p and that ITGA11 was a direct target of miR-516b-5p by luciferase reporter assay. Overall, the present findings demonstrated that FEZF1-AS1 was upregulated and acted as an oncogene

in NSCLC by regulating the ITGA11/miR-516b-5p axis, suggesting that FEZF1-AS1 may be a potential prognostic biomarker and therapeutic target for NSCLC.

Introduction

Lung cancer, as one of the most common types of cancer, causes more deaths than breast, prostate, colorectal and brain cancer combined in 2017 in the United States, with the 5-year relative survival rate being 5% (1). Non-small cell lung cancer (NSCLC) accounted for >80% of all lung cancer cases worldwide in 2016, which fall into several categories, including adenocarcinoma, squamous cell carcinoma and large cell carcinoma (2). The 5-year survival rate for metastatic NSCLC is <5%, and that for patients with early-stage NSCLC is <50% (3). Therefore, finding novel target biomarkers is urgently required.

Accumulating evidence has revealed that most RNA transcripts do not encode proteins in mammals (4,5). Long non-coding RNAs (lncRNAs) are a class of non-coding RNAs of >200 nucleotides in length (6). lncRNAs used to be considered non-functional (7), but an increasing number of lncRNAs have now been reported to serve important roles in biological processes; for example, lncRNAs form extensive networks of ribonucleoprotein complexes with numerous chromatin regulators and then target enzymatic activities to appropriate locations in the genome (8,9). Rigorous evidence has suggested that certain lncRNAs exert important regulatory effects in carcinogenesis and the progression of prostate, hepatocellular and lung cancer, with potential roles in oncogenic or tumor-suppressive signaling pathways (4,10,11-13).

FEZ family zinc finger 1 antisense RNA 1 (FEZF1-AS1) is a lncRNA that is highly expressed in colorectal carcinoma (CRC), and its overexpression can promote the aggressive behavior of CRC cells, both *in vitro* and *in vivo* (14). In gastric cancer, high FEZF1-AS1 expression promotes cell proliferation (14). In addition, the inhibition of FEZF1-AS1 can suppress the activation of the Wnt/ β -catenin signaling pathway (15). Additionally, FEZF1-AS1 expression is upregulated in lung adenocarcinoma and is mediated by FEZF1 (16). However, the mechanism of FEZF1-AS1 in NSCLC remains unclear. Although FEZF1-AS1 expression is upregulated in multiple types of cancer, there are different views on the

Correspondence to: Dr Lingxiao Xing, Department of Pathology, Hebei Medical University, 361 East Zhongshan Road, Shijiazhuang, Hebei 050017, P.R. China
E-mail: xinglingxiao@hotmail.com

Key words: long non-coding RNA, non-small cell lung cancer, microRNA, FEZ family zinc finger 1 antisense RNA 1, integrin subunit $\alpha 11$

location and mechanism of FEZF1-AS1 in the existing literature. He *et al* (17) reported that FEZF1-AS1 is located in the cytoplasm and nucleus in lung adenocarcinoma A549 and SPC-A1 cells, while in other studies FEZF1-AS1 has been reported to be mainly located in the cytoplasm in osteosarcoma, pancreatic ductal adenocarcinoma and myeloma (18-20). Therefore, further elucidation of the mechanism and location of FEZF1-AS1 in NSCLC is required.

In the present study, the association between the expression levels of FEZF1-AS1 in NSCLC tissues and overall survival (OS) was explored. In addition, the function of FEZF1-AS1 in NSCLC cells, the N⁶-methyladenosine (m⁶A) modification and the involvement of the FEZF1-AS1/integrin subunit α 11 (ITGA11)/microRNA (miRNA/miR)-516b-5p axis in NSCLC were investigated. The present results may provide novel biomarkers for NSCLC.

Materials and methods

Patient and clinical data collection. The study protocol was approved by the Institutional Review Board of Hebei Medical University (Shijiazhuang, China). Frozen surgical tumor tissues and corresponding normal lung tissues (5 cm from the edge of the tumor) of 45 patients with NSCLC (including 17 squamous cell carcinoma, 27 adenocarcinoma and 1 atypical carcinoid) were obtained from The Fourth Hospital of Hebei Medical University (Shijiazhuang, China) between February 2009 and February 2018. The median age of the patients was 61 years (range, 44-73 years). All patients were diagnosed with NSCLC on histopathological evaluation, and were reviewed by experienced pathologists and staged according to the 8th edition lung cancer classification of the American Joint Committee of Cancer (21). EGFR was detected via PCR, and ALK was detected via fluorescence *in situ* hybridization (FISH) by the Department of Pathology of the Fourth Hospital of Hebei Medical University. PD-1 and PD-L1 were detected via immunohistochemistry (IHC) by the Department of Pathology of the Fourth Hospital of Hebei Medical University. PCR, FISH and IHC were performed according to routine hospital protocols. No patients received any other treatment prior to surgery, and all patients were followed up until February 2020. The smoking index was calculated as cigarettes/day x smoking time (years). Since a smoking index ≥ 400 indicated a high risk of lung cancer, patients were divided into never smokers (0, smoking index=0), light smokers (1, smoking index <400) and heavy smokers (2, smoking index ≥ 400). The study was conducted in accordance with the Declaration of Helsinki, and approval was obtained from the Research Ethics Committee of the Fourth Hospital of Hebei Medical University.

Cell culture. Human NSCLC H358, H1299, A549, H520, SK-MES-1, H1703 and normal human bronchial epithelial BEAS-2B cells were purchased from the China Infrastructure of Cell Line Resources. SK-MES-1 cells were cultured in Minimum Essential Medium (Thermo Fisher Scientific, Inc.) supplemented with 10% FBS (Gemini Bio Products), 10,000 U/ml penicillin and 10,000 μ g/ml streptomycin (Thermo Fisher Scientific, Inc.). H520 cells were cultured in DMEM (Thermo Fisher Scientific, Inc.) supplemented with 10% FBS (Gemini Bio Products), 10,000 U/ml penicillin

and 10,000 μ g/ml streptomycin (Thermo Fisher Scientific, Inc.). The other cells were cultured in RPMI-1640 medium (Thermo Fisher Scientific, Inc.) supplemented with 10% FBS, 10,000 U/ml penicillin and 10,000 μ g/ml streptomycin. BEAS-2B cells were cultured in Bronchial Epithelial Cell Medium (ScienCell Research Laboratories, Inc.) with 1% cell growth supplements (cat. no. 3962; ScienCell Research Laboratories, Inc.) and 1% penicillin/streptomycin (Thermo Fisher Scientific, Inc.). All cells were incubated at 37°C with 5% CO₂.

RNA isolation and reverse transcription-quantitative PCR (RT-qPCR). Total RNA from frozen tissues or cultured cells was extracted using TRIzol[®] reagent (Thermo Fisher Scientific, Inc.), according to the manufacturer's protocol. Total RNA (500 ng) was reverse transcribed in a 10- μ l reaction volume, using random primers according to the manufacturer's protocol of the ReverTra Ace[™] qPCR RT Master mix with gDNA Remover kit (Toyobo Life Science). The primer sequences for lncRNA and mRNA expression are shown in Table I. qPCR was performed on the obtained cDNA using SYBR Green (Promega Corporation) following the manufacturer's protocol. PCR was performed using a Gene Amp PCR System MX3005P (Agilent Technologies, Inc.) with the following protocol: 94°C for 5 min, followed by 40 cycles of denaturation at 94°C for 15 sec and annealing/extension at 60°C for 1 min, and a final extension step at 72°C for 5 min. β -actin was used as the reference gene. Analysis of relative gene expression was performed using the 2^{- $\Delta\Delta$ C_q} method (22).

Small interfering RNA (siRNA) silencing and miRNA mimics. H1299 and H520 cells were transfected with siRNA (si-NC, si-FEZF1-AS1, si-ITGA11-1, si-ITGA11-2, si-ITGA11-3, si-METTL3, si-METTL14, si-YTHDF1 and si-YTHDF2; 40 pmol/well; Shanghai GenePharma Co., Ltd.) or miRNA mimics (NC mimics and miR-516b-5p mimics, miR-126a mimics, miR-29b mimics, miR-145 mimics, miR-486 mimics, miR-584 mimics; 100 nmol; Guangzhou RiboBio Co., Ltd.) using Lipofectamine[®] 2000 (Thermo Fisher Scientific, Inc.) and incubated at 37°C with 5% CO₂ for 48 h before subsequent experiments. The siRNA and miRNA mimic sequences are shown in Table II.

Plasmid transfection. The pcDNA-3.1-NC and pcDNA3.1-FEZF1-AS1 plasmids for FEZF1-AS1 overexpression were purchased from GenScript. The plasmids (1 μ g/well) were transfected into H1299 and H520 cells using Lipofectamine 2000 according to the manufacturer's protocol.

Rescue assays. Cells were divided into 4 groups for transfection, which were NC, pcDNA3.1-FEZF1-AS1 only, miR-516b-5p mimics only and pcDNA3.1-FEZF1-AS1 plus miR-516b-5p mimics co-transfection, performed as aforementioned. Cells were harvested after 48 h of transfection.

Cell viability assay. Transfected cells (H1299 and H520) were seeded onto 96-well plates at a density of 1.5x10⁴ cells/well after 8 h of transfection. The cell viability was evaluated every 24 h using a Cell Counting Kit-8 (CCK-8; Dojindo Molecular Technologies, Inc.) assay, following the manufacturer's protocol.

Table I. Primer sequences used for reverse transcription-quantitative PCR.

| Gene | Sequence (5'-3') |
|------------------------|------------------------|
| FEZF1-AS1 forward | ACCTGCCTTCTTACTGAATG |
| FEZF1-AS1 reverse | GCAGTAACCATAGCCAGAAACT |
| YTHDF1 forward | GTGGACACCCAGAGAACAAA |
| YTHDF1 reverse | CAGTAAGGTAGGGCTCAAAGTC |
| YTHDF2 forward | ACAGCCAAGGCCAATAA |
| YTHDF2 reverse | GCAGCTTCACCCAAAGAATAG |
| METTL3 forward | CACTGATGCTGTGTCCATCT |
| METTL3 reverse | CTTGTAGGAGACCTCGCTTTAC |
| METTL14 forward | GAAACTGGCATCACTGCTAATG |
| METTL14 reverse | CCAGAACCACACCAGAGAAA |
| ITGA11 forward | CCTACAGCACGGTCTAAATATC |
| ITGA11 reverse | CTCCTCGTTCACACTCAAT |
| GAPDH forward | GCACCGTCAAGGCTGAGAAC |
| GAPDH reverse | GCCTTCTCCATGGTGGTGAA |
| MALAT1 forward | GCTCAGTTGCGTAATGGAAAG |
| MALAT1 reverse | GTGTTCTCTTGAGGGACAGTAG |
| RHOV forward | ACACCTTCTCTGTGCAAGTC |
| RHOV reverse | GGGAACGAAGTCGGTCAAA |
| ONECUT2 forward | ATGTGGAAGTGGCTTCAGG |
| ONECUT2 reverse | GGGACTTCTTCTGGGAATTGT |
| SOX4 forward | CAGCGACAAGATCCCTTTCA |
| SOX4 reverse | GCCGGACTTCACCTTCTTC |
| MARK4 forward | GGGAGGTTGCCATCAAGATTAT |
| MARK4 reverse | CAGCGTCTTCTCAGTCTCAATC |
| UBN1 forward | CCCAGAGCTGGTGAAGAATATC |
| UBN1 reverse | GGGCTCTACTTTATGCCTTT |
| COL1A1 forward | CTAAAGGCGAACCTGGTGAT |
| COL1A1 reverse | TCCAGGAGCACCAACATTAC |
| PRKAB2 forward | AGCACCAAGATTCCACTGATTA |
| PRKAB2 reverse | CCACTGTCCATCCACAAAGA |
| PIP5K1A forward | CGGCCCGATGATTACTTGTAT |
| PIP5K1A reverse | CGTCGCTGGACACATAGAATAG |
| CDK6 forward | GGATAAAGTTCAGAGCCTGGAG |
| CDK6 reverse | GCGATGCACTACTCGGTGTGAA |
| SKA3 forward | AATCTGCTCAGAACACCTACAC |
| SKA3 reverse | TGGGTGGCACTGCTTTAAT |
| XKR9 forward | AGGCTGCCCAACTTATTC |
| XKR9 reverse | AGAAATAGCACAGCAAGAGACC |
| β -actin forward | AGCGAGCATCCCCAAAGTT |
| β -actin reverse | GGGCACGAAGGCTCATCATT |

FEZF1-AS1, FEZ family zinc finger 1 antisense RNA 1; ITGA11, integrin subunit α 11; MALAT1, metastasis-associated lung adenocarcinoma transcript 1; METTL3/14, methyltransferase-like 3/14; YTHDF1/2, YTH N6-methyladenosine RNA binding protein 1/2.

Cell migration and invasion assay. H1299 and H520 cells were plated in their respective medium (RPMI-1640 and DMEM, respectively) with 1% FBS in the upper chamber of Transwell inserts (8.0- μ m pores; Corning, Inc.). For the migration assays,

Table II. siRNA and miRNA mimics sequences.

| siRNA | Sequence (5'-3') |
|---------------------------------|------------------------|
| si-NC | UUCUCCGAACGUGUCACGUTT |
| si-FEZF1-AS1 | GCAAUAGGCCUGGGAAAGUTT |
| si-METTL3 | CTGCAAGTATGTTCACTATGA |
| si-METTL14 | AAGGATGAGTTAATAGCTAAA |
| si-YTHDF1 | CCGCGTCTAGTTGTTTCATGAA |
| si-YTHDF2 | TTGGCTATTGGGAACGTCCTT |
| si-ITGA11-1 | CCCAGUGGUUCAGAUCAAUTT |
| si-ITGA11-2 | GACGGCAUUUGGCAUUGAATT |
| si-ITGA11-3 | GACCUUCUCAGUCGAGUAUTT |
| Biotinylated-miR-516b-mutated | AGUCAACAGUAAGAAGCACUUU |
| Biotinylated-miR-516b-wild-type | AUCUGGAGGUAAGAAGCACUUU |
| Biotinylated-miR-NC | UUGUACUACACAAAAGUACUG |

FEZF1-AS1, FEZ family zinc finger 1 antisense RNA 1; ITGA11, integrin subunit α 11; siRNA, small interfering RNA; miR/miRNA, microRNA; NC, negative control.

the cells (5×10^4) were suspended in 200 μ l RPMI-1640 medium or DMEM in the upper chamber. For the invasion assays, the cells (2×10^5) were suspended in 200 μ l RPMI-1640 medium or DMEM, and placed into the upper chamber (precoated with Matrigel at 37°C for 1 h; Merck KGaA). The bottom chamber contained medium with 10% FBS. Following incubation at 37°C for 48 h, the cells that had migrated or invaded through the membrane were fixed with 4% formaldehyde for 30 min at room temperature, stained with 0.5% crystal violet for 8 min at room temperature and imaged using a light microscope at a magnification of x400.

Cell cycle analysis. The cells were collected by centrifugation at 160 x g at 4°C for 5 min and washed twice with cold PBS. For cell cycle analysis, the cells were fixed overnight in 70% ethanol at 4°C. Following centrifugation for 5 min at 160 x g at 4°C, the pellet was stained with 50 μ g/ml propidium iodide (BD Biosciences) in 0.1% Triton X-100, 100 μ g/ml RNase A (Thermo Fisher Scientific, Inc.) and 0.02 mg/ml EDTA. Cell suspensions were analyzed via flow cytometry using a FACSCalibur system (BD Biosciences). The cell cycle distribution was analyzed using Flow Jo 7.6 software (FlowJo LLC).

Coding potential tool. The coding potential of FEZF1-AS1 was calculated using the Coding-Potential Assessment Tool (lilab.research.bcm.edu/cpat/).

m⁶A prediction and analysis. The sequence-based RNA adenosine methylation site predictor (SRAMP) software (<http://www.cuilab.cn/sramp>) was used for m⁶A prediction and analysis (23). Treatment with 3-Deazaadenosine can cause tumor cells to be in an RNA demethylation state (24). Therefore, H1299 cells were incubated with 10 μ M 3-Deazaadenosine at 37°C for 4 or 24 h.

Subcellular fractionation. The Minute Cytoplasmic and Nuclear Extraction kit (Invent Biotechnologies, Inc.) was used to extract cytoplasmic and nuclear fractions from NSCLC cell lines, following the manufacturer's protocol. The RNA was extracted using TRIzol reagent, as aforementioned. Subsequently, RT-qPCR was performed as aforementioned to evaluate the expression levels of each fraction of nuclear control transcript [metastasis-associated lung adenocarcinoma transcript 1 (MALAT1)], cytoplasmic control transcript (GAPDH) and FEZF1-AS1.

Western blot analysis. Total protein was extracted from cell lines using freshly prepared RIPA lysis buffer (150 mM NaCl, 1% NP-40, 0.1% SDS, 2 μ g/ml Aprotinin, 2 μ g/ml Leupeptin, 1 mM PMSF, 1.5 mM EDTA, 1 mM NaVanadate) and protein concentration was determined using a BCA assay. A total of 40 μ g protein/lane was separated via 15% SDS-PAGE and transferred electrophoretically to nitrocellulose membranes. To evaluate protein expression, the blots were blocked with 5% skimmed milk in TBS with 0.05% Tween-20 at 37°C for 1.5 h and incubated at 4°C overnight with a primary rabbit monoclonal antibody against ITGA11 (1:1,000; cat. no. ab198826; Abcam) and an antibody against β -actin (1:10,000; cat. no. ac009; ABclonal Biotech Co., Ltd.) used as a control. The blots were then probed with HRP-conjugated goat anti-rabbit (1:5,000; cat. no. sc-2004; Santa Cruz Biotechnology, Inc.) or anti-mouse (1:8,000; cat. no. sc-2005; Santa Cruz Biotechnology, Inc.) secondary antibodies at 37°C for 1.5 h, visualized using enhanced chemiluminescence (Thermo Fisher Scientific, Inc.) and scanned using ImageQuant LAS 4010 Imaging System (GE Healthcare Life Sciences).

RNA-binding protein immunoprecipitation (RIP). RIP experiments were performed using the Magna RIP RNA-binding protein immunoprecipitation kit (EMD Millipore) and anti-argonaute 2 (Ago2) antibody (5 μ g; cat. no. ab32381; Abcam), according to the manufacturer's protocol. Purified, co-precipitated RNAs were subjected to RT-qPCR analysis, as aforementioned.

RNA pulldown assay with biotinylated miRNA. H1299 cells were transfected with biotinylated miRNAs (30 nM; Table II) as aforementioned, and harvested 48 h after transfection. The cell lysates were incubated at 4°C for 6 h with M-280 streptavidin magnetic beads (Thermo Fisher Scientific, Inc.) as previously described (25). The bound RNAs were purified using TRIzol reagent for further RT-qPCR analysis as aforementioned.

Luciferase reporter assay. To create a 3'-untranslated region (UTR) luciferase reporter construct of ITGA11, the sequences from putative miR-516b-5p binding sites were synthesized and cloned into the pmirGLO vector (Promega Corporation). The following wild-type (WT) and mutated (MUT) primers were used to construct the 3'-UTR of ITGA11: WT forward, 5'-ACTCGAGcccagcaatggcgcctgctccctccagaatggaactcaagctgttAGATC-3' and WT reverse, 5'-CGCGTGAGCTCgggctcttaccgaggacagggaggtcttaccttgagttcgaccaaT-3'; MUT forward, 5'-ACTCGAGcccagcaatggcgcctgctccagaactcatggaactcaagctgg

ttAGATC-3' and MUT reverse, 5'-CGCGTGAGCTCgggctcttaccgaggacagggaggtcttaccttgagttcgaccaaT-3'. The amplified fragment was cloned into the pmirGLO luciferase reporter vector at the *MluI* and *XbaI* sites. Briefly, cancer cells (5×10^4 per well) were seeded in a 24-well plate the day before transfection, and then co-transfected using Lipofectamine[®] 2000 (Thermo Fisher Scientific, Inc.) with the firefly luciferase-3'-UTR (pmirGLO or pmirGLO-ITGA11; 500 ng), along with miR-516b-5p or control mimics (Guangzhou RiboBio Co., Ltd.). After 48 h, luciferase activity was measured using the Luc-Pair[™] Duo-Luciferase HS assay kit (GeneCopoeia, Inc.) and normalized to the *Renilla* luciferase activity. All experiments were repeated at least three times.

Microarray analysis. Arraystar Human LncRNA Microarray V4.0 (Kangchen BioTech Co., Ltd.) was used to screen the global profiling of human lncRNAs and protein-coding transcripts. The samples included eight frozen tissues of NSCLCs (four samples of squamous cell carcinoma and four of adenocarcinoma) and paired normal lung tissues (GSE137445) (26). The total RNA was extracted from the cells or tissues as aforementioned. Sample labeling and array hybridization were performed according to the Agilent One-Color Microarray-Based Gene Expression Analysis protocol (Agilent Technologies, Inc.) with minor modifications. Briefly, mRNA was purified from total RNA after removal of ribosomal RNA (mRNA-ONLY[™] Eukaryotic mRNA Isolation kit; Epicentre; Illumina, Inc.). Subsequently, each sample was amplified and transcribed into fluorescent cRNA along the entire length of the transcripts without 3' bias utilizing a random priming method (Arraystar Flash RNA Labeling kit; Arraystar, Inc.). The labeled cRNAs were purified using an RNeasy Mini kit (Qiagen, Inc.). The concentration and specific activity of the labeled cRNAs (pmol Cy3/ μ g cRNA) were measured by NanoDrop ND-1000 (Thermo Fisher Scientific, Inc.). A total of 1 μ g of each labeled cRNA was fragmented by adding 5 μ l 10X blocking agent and 1 μ l 25X fragmentation buffer; the mixture was heated at 60°C for 30 min, and finally 25 μ l 2X GE hybridization buffer was added to dilute the labeled cRNA. A total of 50 μ l hybridization solution was dispensed into the gasket slide and assembled to the LncRNA expression microarray slide. The slides were incubated for 17 h at 65°C in an Agilent Hybridization Oven (Agilent Technologies, Inc.). The hybridized arrays were washed, fixed and scanned using the Agilent DNA Microarray Scanner (part no. G2505C; Agilent Technologies, Inc.). Quantile normalization and subsequent data processing were performed using the GeneSpring GX v11.5.1 software package (Agilent Technologies, Inc.). The thresholds used to screen the upregulated or downregulated lncRNAs were fold-change (FC) ≥ 2.0 and $P \leq 0.05$. In addition, the competing endogenous (ce)RNA network of FEZF1-AS1 was analyzed by integrating the Arraystar Human mRNA microarray data and miRNA bioinformatic analysis software (TargetScan v7.2; <http://www.microrna.org>) by Kangchen BioTech Co., Ltd..

Statistical analysis. All data are presented as the mean \pm SEM. All experiments were repeated ≥ 3 times. SPSS 22.0 (IBM Corp.) was used for statistical analysis. The association between the expression levels of FEZF1-AS1, ITGA11 and

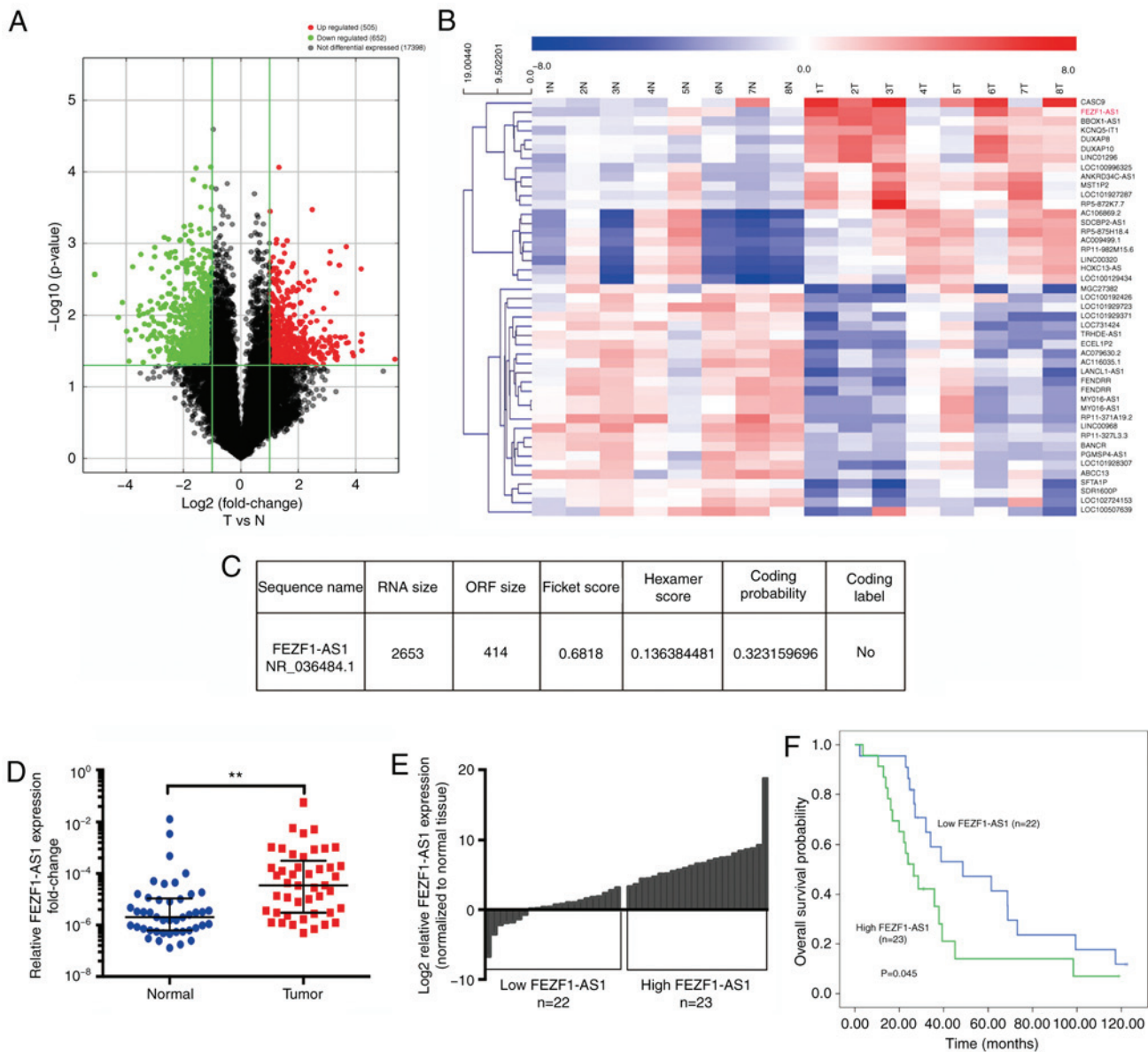


Figure 1. FEZF1-AS1 is upregulated in NSCLC tissues and is associated with a poor prognosis. (A) Volcano plot of lncRNAs in NSCLC compared with non-tumorous tissues (defined by $FC \geq 2$ and $P < 0.05$). (B) Heat map when limited by $FC \geq 5$ and $P < 0.05$. FEZF1-AS1 was one of the most upregulated lncRNAs. Blue scale represents downregulation and red scale represents upregulation. (C) FEZF1-AS1 had no coding ability according to the Coding-Potential Assessment Tool. (D) Reverse transcription-quantitative PCR analysis of FEZF1-AS1 expression in 45 pairs of NSCLC tissues and corresponding non-tumor lung tissues. (E) Patients were divided into high ($FC > 9.00$; $n=23$) or low ($FC \leq 9.00$; $n=22$) FEZF1-AS1 expression groups according to the median of FEZF1-AS1 expression. (F) Patients with high FEZF1-AS1 expression had a shorter overall survival rate than patients with low FEZF1-AS1 expression ($P=0.045$). Data are presented as the mean \pm SEM. $**P < 0.01$. NSCLC, non-small cell lung cancer; FC, fold change; lncRNAs, long non-coding RNAs; FEZF1-AS1, FEZ family zinc finger 1 antisense RNA 1; ORF, open reading frame.

miR-516b-5p, and the clinicopathological variables of patients with NSCLC was determined using the χ^2 test. Paired t-test was used to examine the expression levels of FEZF1-AS1, ITGA11 and miR-516b-5p in normal versus tumor tissue samples. Unpaired t-test was utilized to examine the differences between two groups *in vitro*. Significant differences among multiple groups were investigated using one-way ANOVA followed by Bonferroni's post hoc test. Kaplan-Meier analysis with log-rank test was used to assess the overall survival rate. The correlation between FEZF1-AS1, ITGA11 and miR-516b-5p expression in NSCLC tissues was analyzed using Spearman's correlation analysis. $P < 0.05$ was considered to indicate a statistically significant difference.

Results

FEZF1-AS1 is upregulated in NSCLC tissues and is associated with a poor prognosis. To identify the regulatory networks of mRNA and lncRNAs in NSCLC, eight pairs of NSCLC and non-tumorous adjacent tissues, including four pairs of adenocarcinoma and four pairs of squamous cell carcinoma, were analyzed using the Arraystar Human lncRNA microarray. A total of 1,157 lncRNAs were found to be significantly differentially expressed, of which 505 were upregulated and 652 were downregulated by >2 -fold (Fig. 1A). With the further restriction of $FC \geq 5$ and $P < 0.05$, FEZF1-AS1 was one of the most upregulated lncRNAs (Fig. 1B), suggesting the

Table III. Association between low (n=22) and high (n=23) FEZF1-AS1 expression and clinicopathological features in patients with non-small cell lung cancer.

| Parameter | FEZF1-AS1 expression, n (%) | | P-value |
|------------------------------|-----------------------------|-----------|---------|
| | Low | High | |
| Age, years | | | >0.999 |
| <60 | 11 (47.8) | 12 (52.2) | |
| ≥60 | 11 (50.0) | 11 (50.0) | |
| Sex | | | 0.722 |
| Male | 18 (51.4) | 17 (48.6) | |
| Female | 4 (40.0) | 6 (60.0) | |
| Smoking history ^a | | | 0.867 |
| Never | 7 (46.7) | 8 (53.3) | |
| Light | 2 (40.0) | 3 (60.0) | |
| Heavy | 13 (52.0) | 12 (48.0) | |
| Family history | | | 0.090 |
| No | 21 (53.8) | 18 (46.2) | |
| Yes | 1 (16.7) | 5 (83.3) | |
| Tumor size, cm | | | 0.542 |
| ≤5 | 13 (44.8) | 16 (55.2) | |
| >5 | 9 (56.3) | 7 (43.8) | |
| Lymph node metastasis | | | >0.999 |
| Negative | 11 (47.8) | 12 (52.2) | |
| Positive | 11 (50.0) | 11 (50.0) | |
| Stage ^b | | | >0.999 |
| I-II | 10 (47.6) | 11 (52.4) | |
| III-IV | 12 (50.0) | 12 (50.0) | |

^aSmoking index=cigarette/day x smoking time (years). Since a smoking index ≥400 indicated high risk of lung cancer, patients were divided into never smokers (smoking index=0), light smokers (smoking index <400) and heavy smokers (smoking index ≥400). ^bStage was determined according to the 8th edition lung cancer classification of the American Joint Committee of Cancer. FEZF1-AS1, FEZ family zinc finger 1 antisense RNA 1.

potential crucial role of FEZF1-AS1 in NSCLC tumorigenesis and development. The coding potential of FEZF1-AS1 was calculated using the Coding-Potential Assessment Tool (lilab.research.bcm.edu/cpat/), revealing that the possible open reading frame of FEZF1-AS1 was very short, with a very low coding probability (Fig. 1C).

To investigate the expression levels of FEZF1-AS1 in NSCLC, RT-qPCR analysis was performed using the total RNA extracted from 45 pairs of NSCLC tissues and their matched non-neoplastic counterparts. The results revealed that FEZF1-AS1 expression was significantly upregulated in NSCLC samples compared with that in the corresponding normal tissues (Fig. 1D). To determine the association between FEZF1-AS1 and clinicopathological features, the 45 patients were divided into the high (FC>9.00; n=23) or low (FC≤9.00; n=22) FEZF1-AS1 expression groups according to the median

of FEZF1-AS1 expression (Fig. 1E). Kaplan-Meier analysis demonstrated that high FEZF1-AS1 expression was significantly associated with a poor OS rate (P=0.045; Fig. 1F). However, there were no significant associations between FEZF1-AS1 expression and other important clinicopathological features, such as lymph node metastasis and clinical staging in patients with NSCLC (all P>0.05; Tables III and SI).

FEZF1-AS1 silencing inhibits lung cancer cell proliferation, migration and invasion. The function of FEZF1-AS1 was investigated in NSCLC cell lines. Compared with BEAS-2B cells, FEZF1-AS1 expression was significantly upregulated in H358, H1299, H520 and SK-MES-1 NSCLC cells (Fig. 2A). In order to elucidate the mechanism of FEZF1-AS1 activity in oncogenesis, the expression levels of FEZF1-AS1 were further examined in H1299 cells by cytoplasmic and nuclear extraction, revealing that FEZF1-AS1 was mostly located in the cytoplasmic fraction (Fig. 2B). To investigate the biological function of FEZF1-AS1, knockdown efficiency of si-FEZF1-AS1 was measured using RT-qPCR in H1299 and H520 cells (Fig. 2C). The CCK-8 assay revealed that FEZF1-AS1-knockdown significantly decreased the proliferative capacity of NSCLC cells after ≥72 h (Fig. 2D). Additionally, it was observed that FEZF1-AS1 silencing induced G₂/M arrest (Figs. 2E and S1A), and Transwell assays demonstrated that migration and invasion were significantly inhibited following FEZF1-AS1 silencing (Fig. 2F and G).

High FEZF1-AS1 expression in NSCLC cells is regulated by m⁶A methylation. To reveal the motif of the high expression levels of FEZF1-AS1 in NSCLC, m⁶A prediction and analysis software SRAMP was used to predict the full-length sequence (2,653 bp) of FEZF1-AS1. As presented in Fig. 3A and B, seven m⁶A modified sites were predicted, suggesting that FEZF1-AS1 expression may be regulated by m⁶A modification.

m⁶A is the most widely used mRNA modification method in mammals; this modification can be added, deleted and preferentially combined with m⁶A through three regulators, including 'writers' that generate m⁶A, 'erasers' that exhibit demethylation activity and 'readers' that decode the m⁶A modification (27). On the basis of this prediction, specific siRNAs targeting the 'readers' [methyltransferase-like 3 (METTL3) and METTL14] and 'writers' [YTH N6-methyladenosine RNA binding protein 1 (YTHDF1) and YTHDF2] were transfected into H1299 cells to examine their effects on FEZF1-AS1 expression. The efficacy of siRNA interference against METTL3, METTL14, YTHDF1 and YTHDF2 was analyzed via RT-qPCR (Fig. 3C). Compared with the control group, downregulating these four m⁶A modified molecules inhibited the expression levels of FEZF1-AS1 (Fig. 3D). Subsequently, H1299 cells were treated with 3-Deazaadenosine, an RNA demethylation drug, at a concentration of 10 μM. FEZF1-AS1 expression was detected in the cells collected at 4 and 24 h following administration. Compared with the control group, FEZF1-AS1 expression was significantly decreased in the 4-h group and reversed in the 24-h group (Fig. 3E). The present results suggested that the high expression levels of FEZF1-AS1 in NSCLC cells was positively regulated by m⁶A methylation.

ITGA11 is a potential target of FEZF1-AS1 through miRNAs in NSCLC cells. FEZF1-AS1 was mostly located in the cytoplasm.

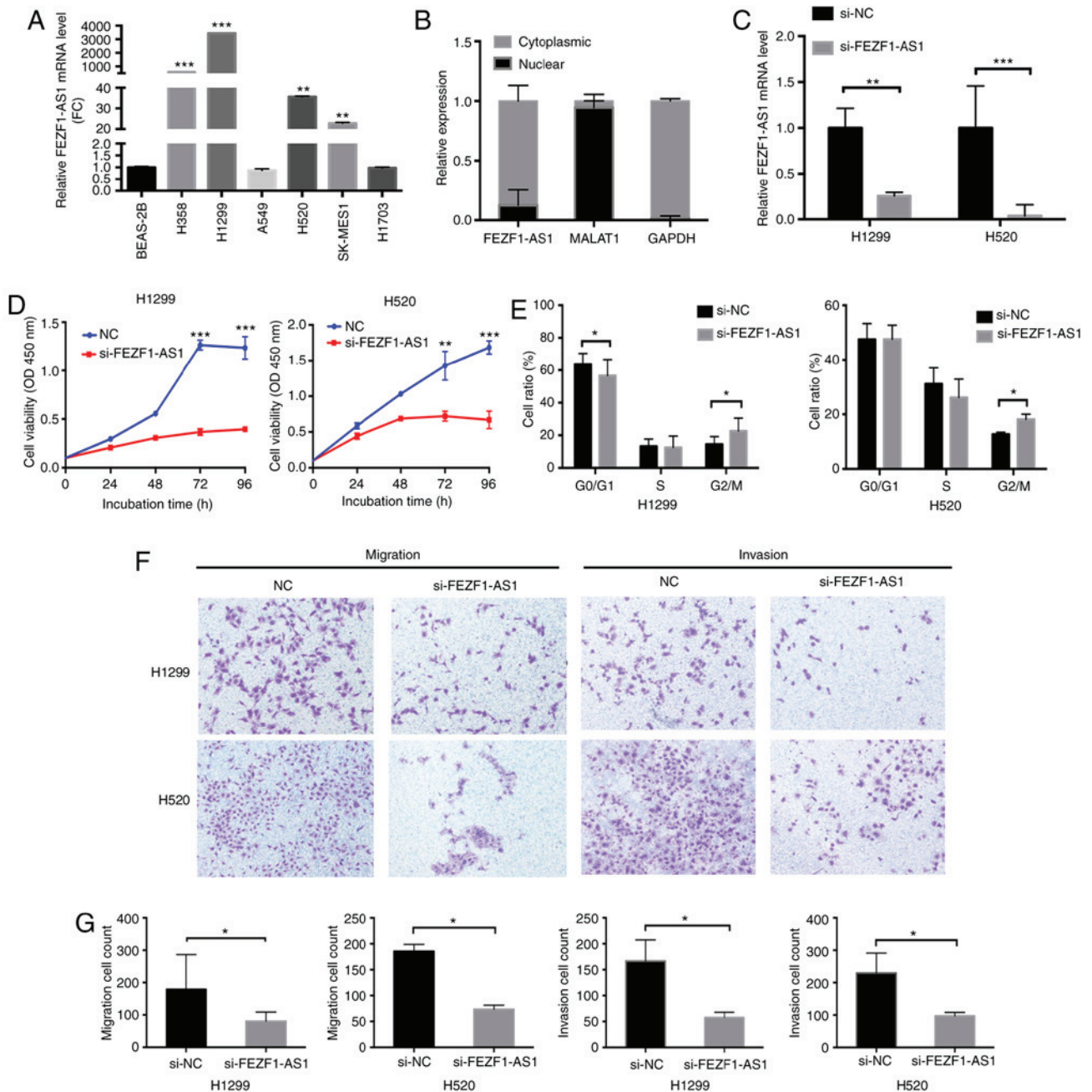


Figure 2. FEZF1-AS1-knockdown inhibits lung cancer cell proliferation, migration and invasion. (A) Reverse transcription-quantitative PCR analysis of FEZF1-AS1 expression in BEAS-2B and six NSCLC cell lines. ** $P < 0.01$ and *** $P < 0.001$ vs. BEAS-2B. (B) Subcellular fractionation revealed that FEZF1-AS1 was mostly located in the cytoplasmic compartment. (C) Efficacy of FEZF1-AS1-knockdown. (D) Growth curves of H1299 and H520 cells following transfection with siFEZF1-AS1 or siNC, as revealed using a Cell Counting Kit-8 assay. (E) FEZF1-AS1-knockdown induced G₂/M arrest in both H1299 and H520 cells. (F and G) FEZF1-AS1-knockdown significantly decreased the migration and invasion of NSCLC cells in the Transwell assays (magnification, x400). Data are presented as the mean \pm SEM. * $P < 0.05$; ** $P < 0.01$; *** $P < 0.001$. NSCLC, non-small cell lung cancer; NC, negative control; si, small interfering; FEZF1-AS1, FEZ family zinc finger 1 antisense RNA 1; MALAT1, metastasis-associated lung adenocarcinoma transcript 1; OD, optical density; FC, fold-change.

It has been demonstrated that lncRNAs in the cytoplasm can interact with miRNAs as ceRNAs (7). Ago2 is a crucial factor in miRNA biogenesis (28). An RIP experiment was performed using an Ago2 antibody to investigate whether FEZF1-AS1 may bind to miRNAs. As expected, FEZF1-AS1 was detected in Ago2 immunoprecipitates from control cells, indicating that the RNA could indeed bind to miRNAs (Fig. 4A).

lncRNAs can regulate miRNAs to influence the expression levels of mRNAs as ceRNAs (8). Combined with the lncRNA microarray and miRNA bioinformatic analysis

using TargetScan software programs results (data not shown), mRNA-ceRNA analysis was performed to identify target genes. Based on the gene frequency, a total of 12 mRNAs (ITGA11, RHOV, ONECUT2, SOX4, MARK4, UBN1, COL1A1, PRKAB2, PIP5K1A, CDK6, SKA3 and XKR9) were selected for further validation. Following the knockdown of FEZF1-AS1, ITGA11 was the most downregulated mRNA, as revealed using RT-qPCR (Fig. 4B). Compared with BEAS-2B cells, the expression levels of ITGA11 were significantly increased in H358, H1299, H520 and SK-MES-1 cells

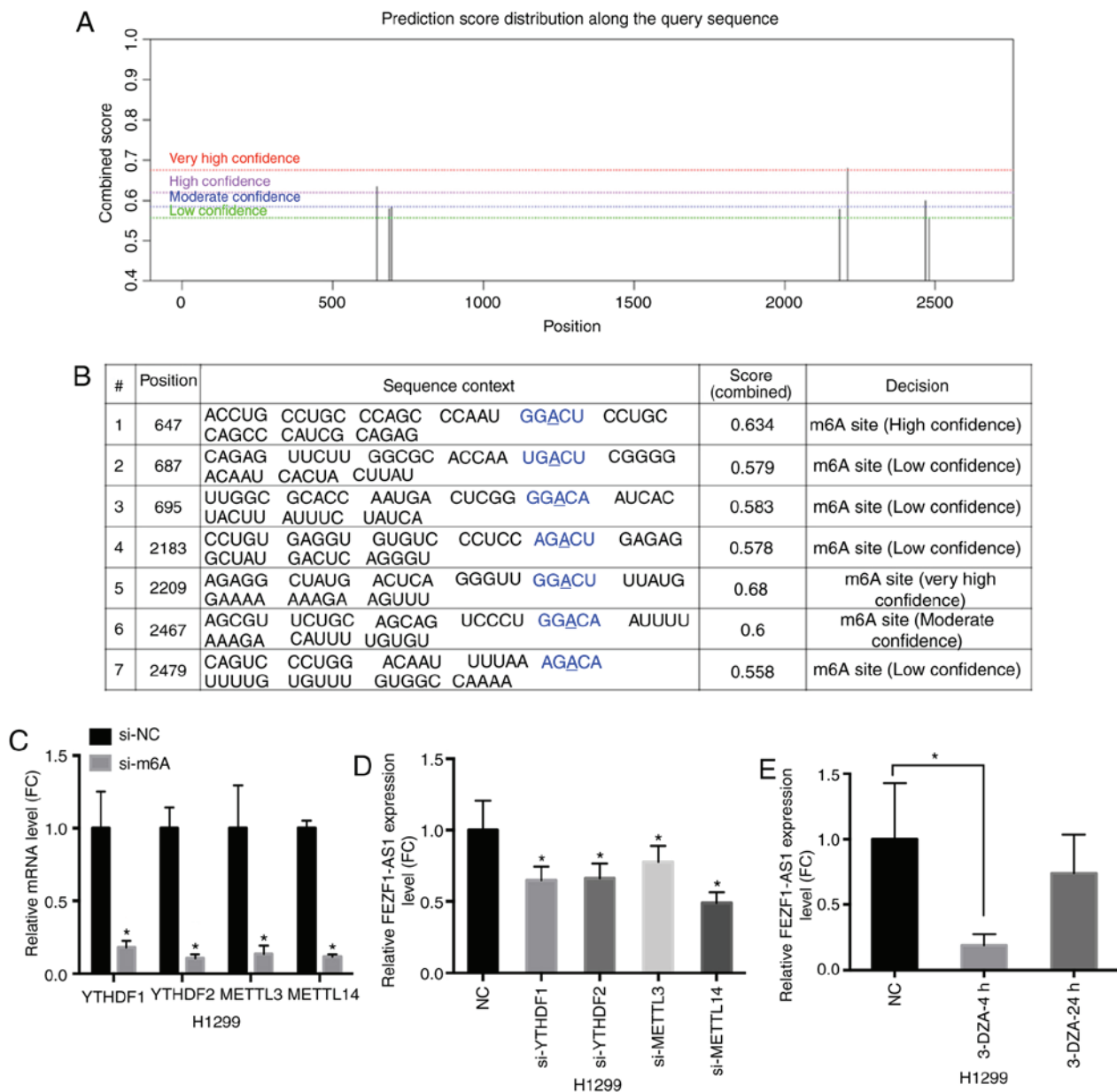


Figure 3. m^6A modification is involved in the high expression levels of FEZF1-AS1. (A) FEZF1-AS1 sequence-based m^6A modification site prediction using the SRAMP software combined with the prediction score. (B) Positions of m^6A modification sites. (C) Knockdown efficiency of m^6A siRNAs specific to YTHDF1, YTHDF2, METTL3 and METTL14 in H1299 cells, and their respective expression levels. (D) FEZF1-AS1 expression in H1299 cells following si-YTHDF1, si-YTHDF2, si-METTL3 and si-METTL14 transfection. (E) FEZF1-AS1 expression in H1299 cells treated with the demethylation drug 3-DZA for 4 or 24 h. Data are presented as the mean \pm SEM. * $P < 0.05$ vs. NC. m^6A , N6-methyladenosine; NC, negative control; si, small interfering; FEZF1-AS1, FEZ family zinc finger 1 antisense RNA 1; METTL3/14, methyltransferase-like 3/14; YTHDF1/2, YTH N6-methyladenosine RNA binding protein 1/2; 3-DZA, 3-Deazaadenosine; FC, fold-change.

(Fig. 4C). Additionally, western blot analysis confirmed that ITGA11 protein levels were decreased following FEZF1-AS1 knockdown in H1299 and H520 cells (Fig. 4D). Subsequently, the role of FEZF1-AS1 overexpression on ITGA11 expression was further investigated. As shown in Fig. 4E-G, FEZF1-AS1 overexpression significantly upregulated ITGA11 expression both at the mRNA and protein levels in H1299 and H520 cells. Therefore, it was concluded that FEZF1-AS1 was able to upregulate ITGA11 expression.

FEZF1-AS1 can compete with miR-516b-5p for direct binding to ITGA11 in NSCLC cells. Based on the present ceRNA networks results and gene ontology analysis in the GSE137445

array dataset, three miRNAs (miR-486, miR-516b-5p and miR-584-3p) binding to both FEZF1-AS1 and ITGA11 were identified. Furthermore, three other miRNAs (miR-126a, miR-29b and miR-145) targeting ITGA11 were selected based on previous reports (29-31). After miRNA overexpression, miR-516b-5p significantly downregulated FEZF1-AS1 expression (Fig. 5A). Proof of transfection was performed for all miRNA mimics (data not shown). Additionally, it was verified that ITGA11 expression was negatively regulated by miR-516b-5p at both the transcriptional (Fig. 5B) and translational (Fig. 5D) levels, as measured using RT-qPCR and western blot analysis, respectively, after verifying that miR-516b-5p was successfully overexpressed in H1299 and

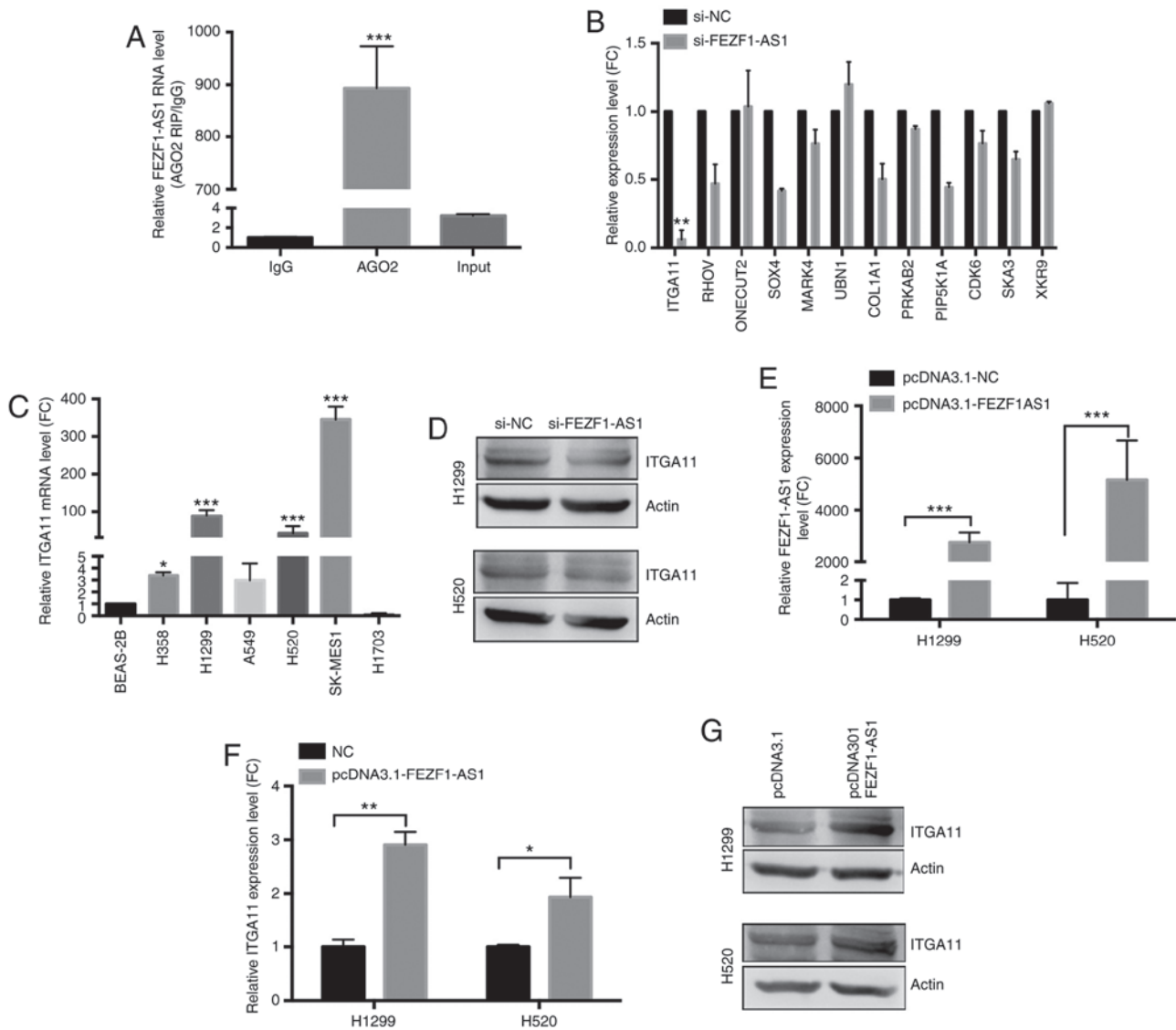


Figure 4. ITGA11 is a potential target of FEZF1-AS1 in NSCLC cells. (A) FEZF1-AS1 was detected in Ago2 immunoprecipitates in the RNA-binding protein immunoprecipitation assay. *** $P < 0.001$ vs. IgG. (B) Following FEZF1-AS1-knockdown, ITGA11 was the most downregulated mRNA of the 12 selected mRNAs, as determined using RT-qPCR. ** $P < 0.01$ vs. si-NC. (C) RT-qPCR analysis of ITGA11 expression in BEAS-2B and NSCLC cell lines. * $P < 0.05$ and *** $P < 0.001$ vs. BEAS-2B. (D) Western blot analysis verified that ITGA11 expression was regulated by FEZF1-AS1. (E) Efficacy of FEZF1-AS1 overexpression. FEZF1-AS1 overexpression upregulated ITGA11 expression, as determined using (F) RT-qPCR and (G) western blot analysis. Data are presented as the mean \pm SEM. * $P < 0.05$; ** $P < 0.01$; *** $P < 0.001$. ITGA11, integrin subunit $\alpha 11$; NSCLC, non-small cell lung cancer; NC, negative control; RT-qPCR, reverse transcription-quantitative PCR; si, small interfering; FEZF1-AS1, FEZ family zinc finger 1 antisense RNA 1; Ago2, argonaute 2; FC, fold-change.

H520 cells (Fig. S1C). Compared with BEAS-2B cells, the expression levels of miR-516b-5p were significantly decreased in H358, H1299, H520, A549 and SK-MES-1 cells (Fig. 5C). Subsequently, it was examined whether miR-516b-5p-mediated ITGA11 regulation occurred through direct targeting of miRNA-binding sites in the ITGA11 sequence. According to the bioinformatics analysis using TargetScan software, the construction diagram of the miR-516b-5p binding site reporter gene in the ITGA11 3'-UTR region (WT and MUT) is shown in Fig. 5E. ITGA11 was subcloned into the pmirGLO dual-luciferase reporter vector, and luciferase assays were performed in H1299 cells by inducing miR-516b-5p overexpression using miR-516b-5p mimics. As shown in Fig. 5F, co-transfection with pmirGLO-ITGA11-WT and miR-516b-5p mimics demonstrated a significant decrease in luciferase reporter activity compared with the negative control (NC)

group ($P < 0.05$). This repressive effect was abolished by directed mutagenesis of the miR-516b-5p binding seed region in ITGA11.

To assess whether miR-516b-5p interacted with FEZF1-AS1, the biotin-avidin pull-down system was used, revealing that FEZF1-AS1 co-precipitated miR-516b-5p (Fig. 5G). For the rescue assay, FEZF1-AS1 and miR-516b-5p were overexpressed either alone or together using transfection. Compared with the NC group, the results revealed that overexpression of miR-516b markedly suppressed ITGA11 expression, whereas overexpression of FEZF1-AS1 partly abolished the silencing effect of miR-516b-5p on ITGA11, suggesting that ITGA11 was regulated by miR-516b-5p and FEZF1-AS1 (Fig. 5H). Therefore, FEZF1-AS1 may function as a ceRNA, regulating miR-516b-5p and its target gene ITGA11 in NSCLC.

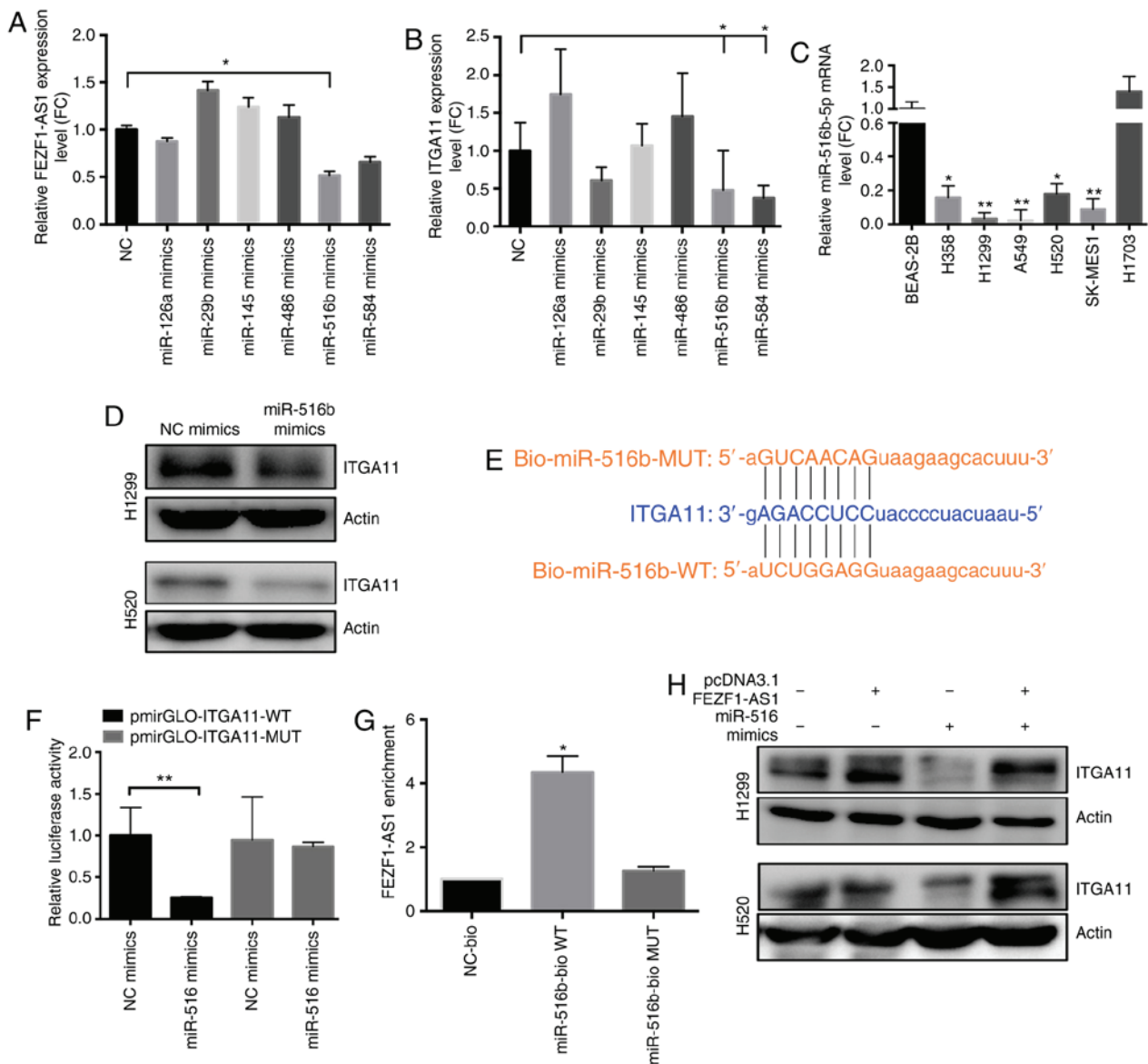


Figure 5. FEZF1-AS1 can compete with miR-516b-5p for direct binding to ITGA11 in NSCLC cells. After miRNA overexpression, miR-516b-5p significantly downregulated (A) FEZF1-AS1 and (B) ITGA11 expression. * $P < 0.05$ vs. NC. (C) miR-516b-5p expression in BEAS-2B and NSCLC cell lines using RT-qPCR. * $P < 0.05$ and ** $P < 0.01$ vs. BEAS-2B. (D) miR-516b-5p overexpression downregulated ITGA11 protein expression, as determined via western blot analysis. (E) Predicted binding site of miR-516b-5p and ITGA11 sequence. (F) Luciferase activity of H1299 cells co-transfected with pmirGLO-ITGA11-WT or pmirGLO-ITGA11-MUT reporter plasmids and miR-516b-5p mimic. (G) Using a biotin-avidin pull-down system, miR-516b-5p precipitated FEZF1-AS1, as determined via RT-qPCR. * $P < 0.05$ vs. NC. (H) Rescue assay supporting the FEZF1-AS1-miR-516b-5p-ITGA11 axis. Data are presented as the mean \pm SEM. NSCLC, non-small cell lung cancer; ITGA11, integrin subunit $\alpha 11$; WT, wild-type; MUT, mutated; NC, negative control; bio, biotinylated; RT-qPCR, reverse transcription-quantitative PCR; miR/miRNA, microRNA; FEZF1-AS1, FEZ family zinc finger 1 antisense RNA 1; FC, fold-change.

Inhibiting ITGA11 or overexpressing miR-516b-5p inhibits cell proliferation and invasion in NSCLC. ITGA11 expression was examined in 45 pairs of NSCLC tissues and their matched non-neoplastic counterparts. It was identified that ITGA11 expression was significantly upregulated in the NSCLC samples compared with that in the corresponding normal tissues (Fig. 6A). To determine the association between ITGA11 and clinicopathological features, the 45 patients were divided into high ($FC > 6.96$; $n = 23$) or low ($FC \leq 6.96$; $n = 22$) ITGA11 expression groups according to the median of ITGA11 expression. However, there were no significant associations between ITGA11 expression and clinicopathological features, such as lymph node metastasis and clinical staging in patients with NSCLC (all $P > 0.05$; Table IV).

To examine the role of ITGA11 in cell proliferation, ITGA11 expression was knocked down in H1299 and H520 cells (Fig. 6B), revealing that the proliferative capacities of these cells were significantly decreased after ≥ 72 h (Fig. 6C). Transwell assays revealed that the knockdown of ITGA11 significantly decreased the migratory and invasive abilities of NSCLC cells (Fig. 6E and F). However, ITGA11-knockdown did not influence the cell cycle (Figs. 6D and S1B).

Compared with surrounding healthy tissues, miR-516b-5p expression was significantly inhibited in tumor tissues compared with in normal tissues (Fig. 7A). To determine the association between miR-516b-5p expression and clinicopathological features, the 45 patients were divided into high ($FC > 0.29$; $n = 23$) or low miR-516b-5p expression groups ($FC \leq 0.29$; $n = 22$).

Table IV. Association between low (n=22) and high (n=23) ITGA11 or miR-516b-5p expression and clinicopathological features in patients with non-small cell lung cancer.

| Parameter | ITGA11 expression, n (%) | | P-value | miR-516b-5p expression, n (%) | | P-value |
|------------------------------|-----------------------------|-----------|---------|----------------------------------|-----------|---------|
| | Low | High | | Low | High | |
| Age, years | | | 0.652 | | | 0.884 |
| <60 | 12 (52.2) | 11 (47.8) | | 11 (47.8) | 12 (52.2) | |
| ≥60 | 10 (45.5) | 12 (54.5) | | 11 (50.0) | 11 (50.0) | |
| Sex | | | 0.936 | | | 0.936 |
| Male | 17 (48.6) | 18 (51.4) | | 17 (48.6) | 18 (51.4) | |
| Female | 5 (50.0) | 5 (50.0) | | 5 (50.0) | 5 (50.0) | |
| Smoking history ^a | | | 0.739 | | | 0.014 |
| Never | 8 (53.3) | 7 (46.7) | | 11 (73.3) | 4 (26.7) | |
| Light | 3 (60.0) | 2 (40.0) | | 0 (0) | 5 (100.0) | |
| Heavy | 11 (44.0) | 14 (56.0) | | 11 (44.0) | 14 (56.0) | |
| Family history | | | 0.413 | | | 0.349 |
| No | 20 (51.3) | 19 (48.7) | | 18 (46.2) | 21 (53.8) | |
| Yes | 2 (33.3) | 4 (66.7) | | 4 (66.7) | 2 (33.3) | |
| Tumor size, cm | | | 0.912 | | | 0.009 |
| ≤5 | 14 (48.3) | 15 (51.7) | | 10 (34.5) | 19 (65.5) | |
| >5 | 8 (50.0) | 8 (50.0) | | 12 (75.0) | 4 (25.0) | |
| Lymph node metastasis | | | 0.181 | | | 0.652 |
| Negative | 9 (39.1) | 14 (60.9) | | 12 (52.2) | 11 (47.8) | |
| Positive | 13 (59.1) | 9 (40.9) | | 10 (45.5) | 12 (54.5) | |
| Stage ^b | | | 0.051 | | | 0.449 |
| I-II | 7 (33.3) | 14 (66.7) | | 9 (42.9) | 12 (57.1) | |
| III-IV | 15 (62.5) | 9 (37.5) | | 13 (54.2) | 11 (45.8) | |

^aSmoking index=cigarette/day x smoking time (years). Since a smoking index ≥400 indicated high risk of lung cancer, patients were divided into never smokers (smoking index =0), light smokers (smoking index <400) and heavy smokers (smoking index ≥400). ^bStage was determined according to the 8th edition lung cancer classification of the American Joint Committee of Cancer. ITGA11, integrin subunit α11; miR, microRNA.

according to the median of miR-516b-5p expression. Smoking history (P=0.014) and tumor size (P=0.009) were associated with miR-516b-5p expression using a χ^2 test in patients with NSCLC (Table IV). However, due to the small sample size of NSCLC tissues, a statistical association between miR-516b-5p expression and OS was not identified (data not shown), nor a correlation between FEZF1-AS1, ITGA11 and miR516b-5p expression (data not shown). The CCK-8 assay revealed that overexpression of miR-516b-5p significantly inhibited NSCLC cell proliferation after ≥72 h (Fig. 7B). Additionally, in the Transwell assay, the migratory and invasive abilities of tumor cells were inhibited in the miR-516b-5p mimic group (Fig. 7C and D) compared with in the control group. The current data indicated that inhibiting ITGA11 or overexpressing miR-516b-5p inhibited cell proliferation and invasion in NSCLC.

Discussion

NSCLC accounts for the vast majority of lung cancer cases (2). In past years, numerous studies regarding non-coding RNAs,

including lncRNAs, have been conducted (4,6-9). lncRNA FEZF1-AS1 is the antisense RNA of FEZF1. In various types of cancer, FEZF1-AS1 expression in cancer tissues is significantly higher compared with that in normal tissues, and high FEZF1-AS1 expression indicates a poor survival in patients with colon, gastric and cervical cancer (15,16,32). The present data revealed that FEZF1-AS1 was highly expressed in NSCLC tissues, compared with normal tissues, and was associated with a poor prognosis in patients with NSCLC. FEZF1-AS1 downregulation in NSCLC cells inhibited cell proliferation, migration and invasion, and arrested the cell cycle at the G₂/M phase, in accordance with findings previously reported on the function of FEZF1-AS1 in NSCLC and breast cancer cell lines (18,33).

Subsequently, the mechanism underlying the high FEZF1-AS1 expression in NSCLC was explored, and m⁶A modification was identified. m⁶A is the most widely used mRNA modification method in mammals (27). The modification can be added, deleted and preferentially combined with m⁶A through three regulators of ‘writers’, ‘erasers’ and

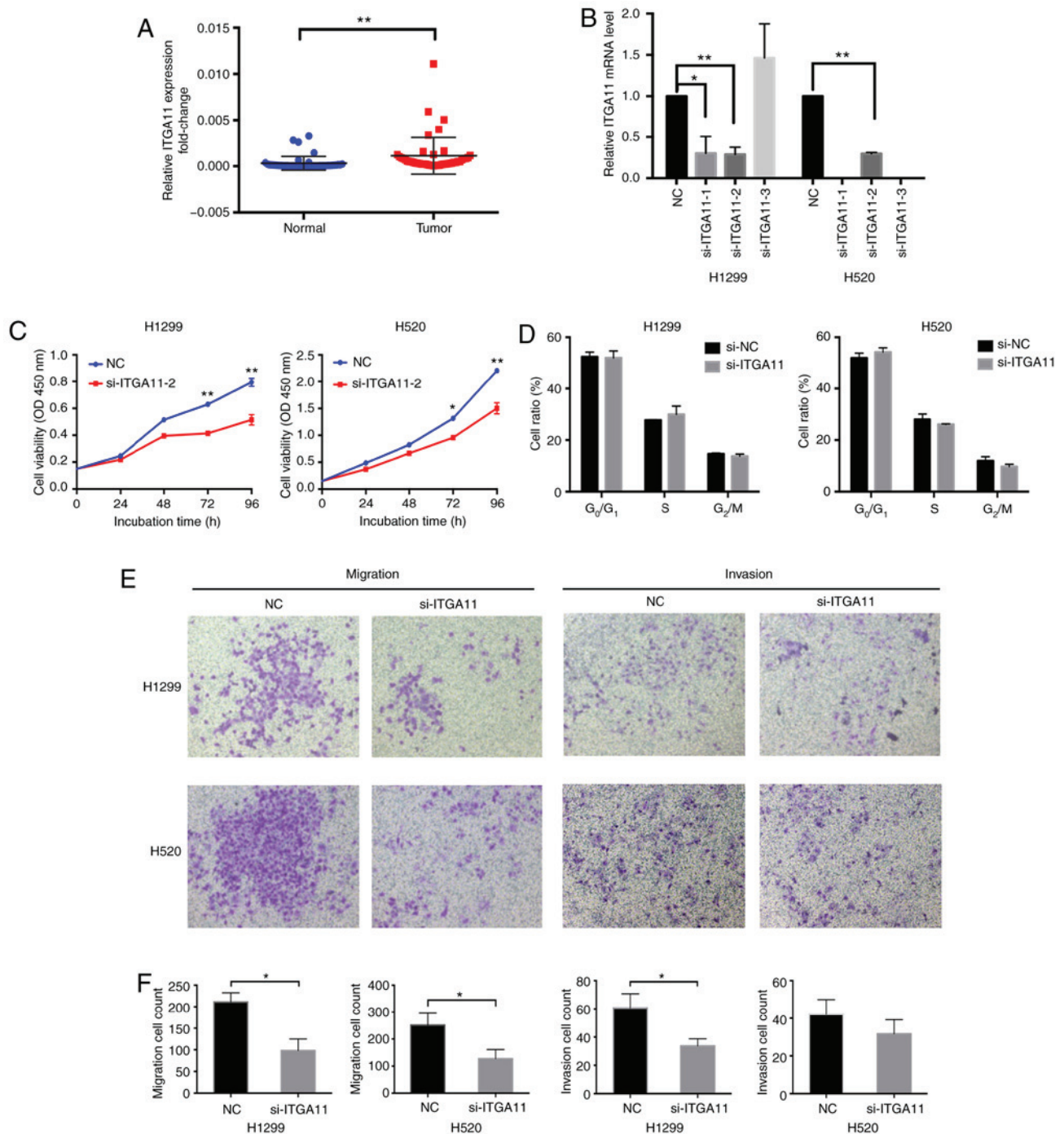


Figure 6. ITGA11 downregulation inhibits cell proliferation and invasion of NSCLC. (A) Reverse transcription-quantitative PCR analysis of ITGA11 expression in 45 pairs of NSCLC tissues and corresponding non-tumor lung tissues analyzing using a paired Student's t-test. (B) ITGA11 downregulation in H1299 and H520 cells. (C) Growth curves of H1299 and H520 cells following transfection with siITGA11 or siNC, as determined using Cell Counting Kit-8 assays. (D) ITGA11-knockdown did not influence the cell cycle. (E and F) Knockdown of ITGA11 significantly decreased the migration and invasion of NSCLC cells in the Transwell assays (magnification, x400). Data are presented as the mean \pm SEM. * $P < 0.05$ and ** $P < 0.01$ vs. NC or indicated groups. NSCLC, non-small cell lung cancer; ITGA11, integrin subunit $\alpha 11$; NC, negative control; si, small interfering; FEZF1-AS1, FEZ family zinc finger 1 antisense RNA 1; OD, optical density.

'readers' (27). The m⁶A modification is involved in a variety of mRNA processes, including mRNA translation and decay (34). In addition to mRNA, non-coding RNAs are also regulated by m⁶A, and miRNAs and lncRNAs are important classes of non-coding RNAs (35). It has been reported in several studies that the expression levels of lncRNAs are regulated by m⁶A modification. For example, the change of lncRNA MALAT1 cut by m⁶A 'reading' molecules is associated with

the progression of cancer (36,37). The downregulation of METTL3 in the 'writing' module can damage the lncRNA Xist-mediated gene silencing (38). However, to the best of our knowledge, whether FEZF1-AS1 expression is regulated by m⁶A modification has not been reported. In the present study, knockdown of 'readers' (METTL3 and METTL14) and 'writers' (YTHDF1 and YTHDF2) resulted in the decrease of FEZF1-AS1 expression. Treatment with 3-Deazaadenosine

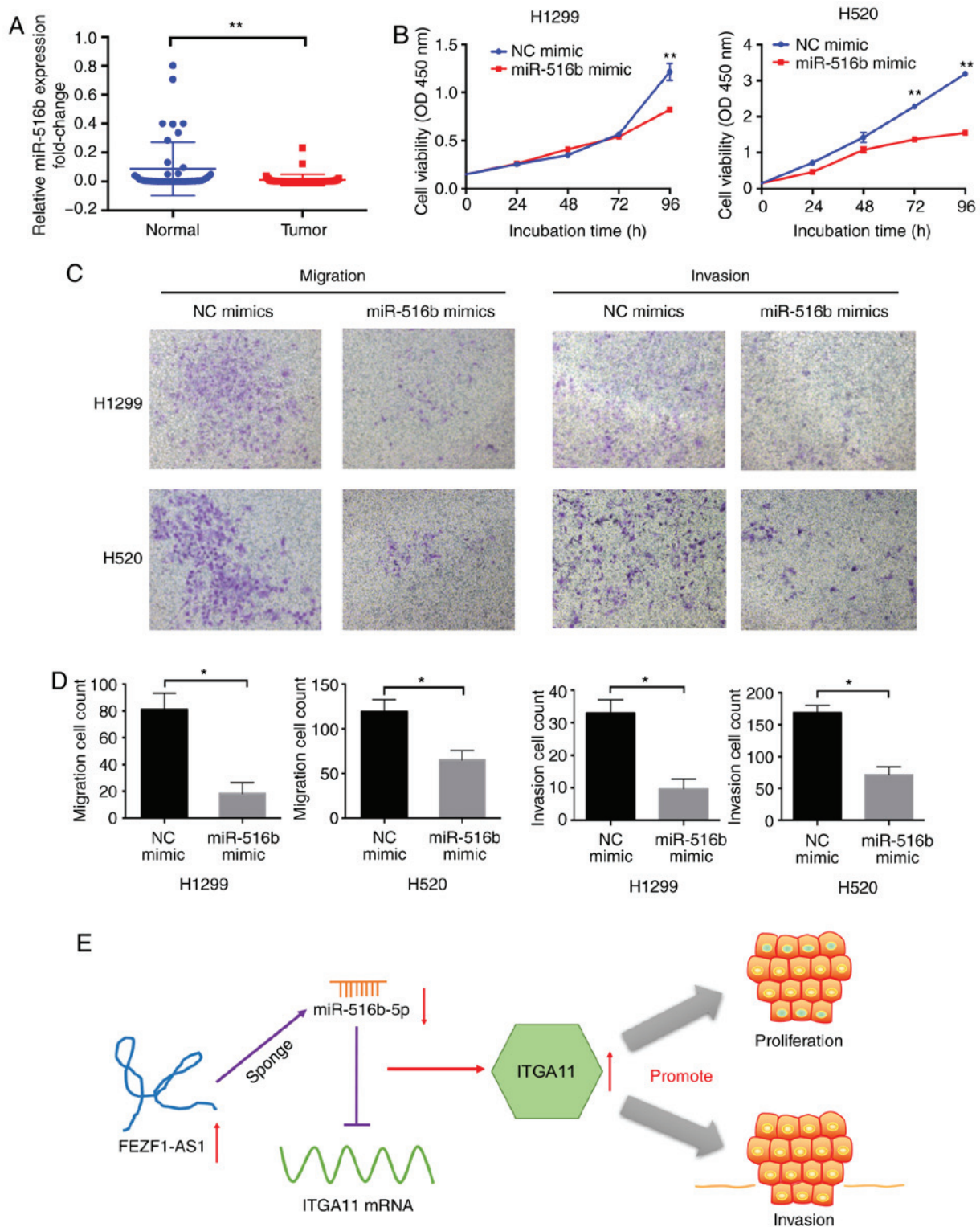


Figure 7. miR-516b-5p overexpression inhibits cell proliferation and invasion in NSCLC. (A) Reverse transcription-quantitative PCR analysis of miR-516b-5p expression in 45 pairs of NSCLC tissues and corresponding non-tumor lung tissues analyzing using a paired Student's t-test. (B) Growth curves of H1299 and H520 cells following miR-516b-5p or NC overexpression were determined using a Cell Counting Kit-8 assay. (C and D) miR-516b-5p upregulation significantly decreased migration and invasion in NSCLC cells in the Transwell assays (magnification, x400). (E) Graph of the potential mechanism of the regulatory network of FEZF1-AS1, miR-516b-5p and ITGA11 in NSCLC cells. FEZF1-AS1 may upregulate ITGA11 via sponging miR-516b-5p, thus promoting the proliferation and invasion of NSCLC cells. Data are presented as the mean \pm SEM. * $P < 0.05$ and ** $P < 0.01$ vs. NC or indicated groups. NSCLC, non-small cell lung cancer; ITGA11, integrin subunit $\alpha 11$; NC, negative control; si, small interfering; FEZF1-AS1, FEZ family zinc finger 1 antisense RNA 1; OD, optical density; miR, microRNA.

causes tumor cells to be in an RNA-demethylation state (24). Following treatment with 3-Deazaadenosine in the present study, FEZF1-AS1 expression was significantly decreased.

The current results demonstrated that m⁶A modification may have an important regulatory effect on FEZF1-AS1 expression.

To investigate the mechanism of FEZF1-AS1 in NSCLC, mRNAs that could be regulated by FEZF1-AS1 were screened, and ITGA11, a member of the integrin family, was selected. Integrins are transmembrane receptors that mediate the connection between cells and their external environment (39). These proteins are heterodimers formed by two subunits, the α (120-185 kD) and β (90-110 kD) subunits (40). In cells, ITGA11 is involved in collagen-mediated biological processes, such as cell migration, collagen deposition and collagen recombination (41). ITGA11 is highly expressed in esophageal squamous cell carcinoma, head and neck squamous carcinoma, prostate cancer and breast cancer, and is closely associated with the migration and invasion of tumor cells (42-44). In lung adenocarcinoma A549, H460 and H520 cell lines, tumor growth was significantly higher in A549+WT, compared with A549+Knockout (KO) tumors (45). Re-expression of human α 11 cDNA in KO cells rescued the tumor growth rate to a rate that was comparable with that of the A549+WT tumors (45). In patients with NSCLC, ITGA11 expression is significantly upregulated and is associated with a poor OS (46). In the present study, both the migration and invasion of NSCLC cells were inhibited following ITGA11-knockdown. This was likely due to the function of integrin in connecting cells to collagen in the extracellular matrix, but this hypothesis needs to be further confirmed.

miR-516b-5p was selected and validated in the present study as a possible binding miRNA to both FEZF1-AS1 and ITGA11. Low miR-516 expression can significantly improve OS in patients with lung squamous cell carcinoma (47). In the present study, miR-516b-5p expression in NSCLC tissues was lower compared with in non-neoplastic tissues, and the proliferation, migration and invasion of cells was inhibited following miR-516b-5p upregulation. In the present study, both ITGA11 and miR-516b-5p were involved in cell proliferation, migration and invasion, which is consistent with the biological role in tumor progression of FEZF1-AS1. Following FEZF1-AS1-knockdown, ITGA11 expression was decreased at both the RNA and protein levels. Additionally, ITGA11 expression was decreased following miR-516b overexpression. Therefore, both FEZF1-AS1 and miR-516b may affect ITGA11 expression. Through RIP and RNA pull-down assays, together with the effects of miR-516b-5p upregulation on FEZF1-AS1, it was concluded that miR-516b-5p and FEZF1-AS1 may share a binding site. The rescue assay further confirmed this regulatory axis (Fig. 7E).

Future studies should explore the effects of silencing both ITGA11 and miR-516b-5p, or of overexpressing FEZF1-AS1 and silencing ITGA11, and to observe phenotypic changes in proliferation and invasion. In addition to the involvement of miR-516b-5p and ITGA11, other FEZF1-AS1-regulated genes may also contribute to the pro-tumorigenic function of FEZF1-AS1. Future studies are warranted to comprehensively explore the role of FEZF1-AS1 in NSCLC pathogenesis.

In conclusion, the present study identified a novel lincRNA, FEZF1-AS1, associated with a poor prognosis in patients with NSCLC. The current results suggested that FEZF1-AS1 was an oncogenic regulator that promoted cell proliferation and invasion. It induced competitive binding with miR-516b-5p, resulting in the upregulation of ITGA11 expression. Therefore, the FEZF1-AS1/miR-516b-5p/ITGA11 axis may be a valuable target for NSCLC prognosis and treatment.

Acknowledgements

Not applicable.

Funding

The present study was supported by Hebei Postgraduate Innovation Funding Project (grant no. CXZZBS2017111).

Availability of data and materials

The datasets used and/or analyzed during the current study are available from the corresponding author on reasonable request.

Authors' contributions

LX designed the study. HeS, HL, XD and ML contributed to cell transfection, RT-qPCR and western blotting. HeS contributed to RIP, RNA pull-down and luciferase assays. HL contributed to data analysis. YL and XZ collected the clinical data and follow-up data. HaS performed the flow cytometric and data analysis. HeS and LX participated in writing and revising the manuscript. All authors have read and approved the final manuscript.

Ethics approval and consent to participate

The research protocol conformed to the principles outlined in the Declaration of Helsinki. All patients provided written informed consent and the protocol of the study was approved by the Research Ethics Committee of the Fourth Hospital of Hebei Medical University.

Patient consent for publication

Not applicable.

Competing interests

The authors declare that they have no competing interests.

References

1. Siegel RL, Miller KD and Jemal A: Cancer statistics, 2020. *CA Cancer J Clin* 70: 7-30, 2020.
2. Bade BC and Dela Cruz CS: Lung cancer 2020: Epidemiology, etiology, and prevention. *Clin Chest Med* 41: 1-24, 2020.
3. Velcheti V, Schalper KA, Carvajal DE, Anagnostou VK, Syrigos KN, Sznol M, Herbst RS, Gettinger SN, Chen L and Rimm DL: Programmed death ligand-1 expression in non-small cell lung cancer. *Lab Invest* 94: 107-116, 2014.
4. Iyer MK, Niknafs YS, Malik R, Singhal U, Sahu A, Hosono Y, Barrette TR, Prensner JR, Evans JR, Zhao S, *et al*: The landscape of long noncoding RNAs in the human transcriptome. *Nat Genet* 47: 199-208, 2015.
5. Djebali S, Davis CA, Merkel A, Dobin A, Lassmann T, Mortazavi A, Tanzer A, Lagarde J, Lin W, Schlesinger F, *et al*: Landscape of transcription in human cells. *Nature* 489: 101-108, 2012.
6. Wang KC and Chang HY: Molecular mechanisms of long noncoding RNAs. *Mol Cell* 43: 904-914, 2011.
7. Ulitsky I and Bartel DP: lincRNAs: Genomics, evolution, and mechanisms. *Cell* 154: 26-46, 2013.
8. Rinn JL and Chang HY: Genome regulation by long noncoding RNAs. *Annu Rev Biochem* 81: 145-166, 2012.

9. Ponting CP, Oliver PL and Reik W: Evolution and functions of long noncoding RNAs. *Cell* 136: 629-641, 2009.
10. Du Z, Sun T, Hacisuleyman E, Fei T, Wang X, Brown M, Rinn JL, Lee MG, Chen Y, Kantoff PW and Liu XS: Integrative analyses reveal a long noncoding RNA-mediated sponge regulatory network in prostate cancer. *Nat Commun* 7: 10982, 2016.
11. Yang Y, Chen L, Gu J, Zhang H, Yuan J, Lian Q, Lv G, Wang S, Wu Y, Yang YT, *et al*: Recurrently deregulated lncRNAs in hepatocellular carcinoma. *Nat Commun* 8: 14421, 2017.
12. Seiler J, Breinig M, Caudron-Herger M, Polycarpou-Schwarz M, Boutros M and Diederichs S: The lncRNA VELUCT strongly regulates viability of lung cancer cells despite its extremely low abundance. *Nucleic Acids Res* 45: 5458-5469, 2017.
13. Park SM, Choi EY, Bae DH, Sohn HA, Kim SY and Kim YJ: The lncRNA EPEL promotes lung cancer cell proliferation through E2F target activation. *Cell Physiol Biochem* 45: 1270-1283, 2018.
14. Chen N, Guo D, Xu Q, Yang M, Wang D, Peng M, Ding Y, Wang S and Zhou J: Long non-coding RNA FEZF1-AS1 facilitates cell proliferation and migration in colorectal carcinoma. *Oncotarget* 7: 11271-11283, 2016.
15. Wu X, Zhang P, Zhu H, Li S, Chen X and Shi L: Long noncoding RNA FEZF1-AS1 indicates a poor prognosis of gastric cancer and promotes tumorigenesis via activation of Wnt signaling pathway. *Biomed Pharmacother* 96: 1103-1108, 2017.
16. Liu Z, Zhao P, Han Y and Lu S: LincRNA FEZF1-AS1 is associated with prognosis in lung adenocarcinoma and promotes cell proliferation, migration and invasion. *Oncol Res* 27: 39-45, 2018.
17. He R, Zhang FH and Shen N: LncRNA FEZF1-AS1 enhances epithelial-mesenchymal transition (EMT) through suppressing E-cadherin and regulating WNT pathway in non-small cell lung cancer (NSCLC). *Biomed Pharmacother* 95: 331-338, 2017.
18. Zhou C, Xu J, Lin J, Lin R, Chen K, Kong J and Shui X: Long noncoding RNA FEZF1-AS1 promotes osteosarcoma progression by regulating the miR-4443/NUPR1 axis. *Oncol Res* 26: 1335-1343, 2018.
19. Ye H, Zhou Q, Zheng S, Li G, Lin Q, Ye L, Wang Y, Wei L, Zhao X, Li W, *et al*: FEZF1-AS1/miR-107/ZNF312B axis facilitates progression and Warburg effect in pancreatic ductal adenocarcinoma. *Cell Death Dis* 9: 34, 2018.
20. Li QY, Chen L, Hu N and Zhao H: Long non-coding RNA FEZF1-AS1 promotes cell growth in multiple myeloma via miR-610/Akt3 axis. *Biomed Pharmacother* 103: 1727-1732, 2018.
21. Goldstraw P, Chansky K, Crowley J, Rami-Porta R, Asamura H, Eberhardt WE, Nicholson AG, Groome P, Mitchell A, Bolejack V, *et al*: The IASLC lung cancer staging project: Proposals for revision of the TNM stage groupings in the forthcoming (Eighth) Edition of the TNM classification for lung cancer. *J Thorac Oncol* 11: 39-51, 2016.
22. Livak KJ and Schmittgen TD: Analysis of relative gene expression data using real-time quantitative PCR and the 2(-Delta Delta C(T)) method. *Methods* 25: 402-408, 2001.
23. Zhou Y, Zeng P, Li YH, Zhang Z and Cui Q: SRAMP: Prediction of mammalian N6-methyladenosine (m6A) sites based on sequence-derived features. *Nucleic Acids Res* 44: e91, 2016.
24. Backlund PS Jr, Carotti D and Cantoni GL: Effects of the S-adenosylhomocysteine hydrolase inhibitors 3-deazaadenosine and 3-deazaaristeromycin on RNA methylation and synthesis. *Eur J Biochem* 160: 245-251, 1986.
25. Wang K, Long B, Zhou LY, Liu F, Zhou QY, Liu CY, Fan YY and Li PF: CARL lncRNA inhibits anoxia-induced mitochondrial fission and apoptosis in cardiomyocytes by impairing miR-539-dependent PHB2 downregulation. *Nat Commun* 5: 3596, 2014.
26. Wang Y, Ding X, Liu B, Li M, Chang Y, Shen H, Xie SM, Xing L and Li Y: ETV4 overexpression promotes progression of non-small cell lung cancer by upregulating PAXN and MMP1 transcriptionally. *Mol Carcinog* 59: 73-86, 2020.
27. Fu Y, Dominissini D, Rechavi G and He C: Gene expression regulation mediated through reversible m⁶A RNA methylation. *Nat Rev Genet* 15: 293-306, 2014.
28. Cheloufi S, Dos Santos CO, Chong MM and Hannon GJ: A dicer-independent miRNA biogenesis pathway that requires Ago catalysis. *Nature* 465: 584-589, 2010.
29. Mao Z, Wu F and Shan Y: Identification of key genes and miRNAs associated with carotid atherosclerosis based on mRNA-seq data. *Medicine (Baltimore)* 97: e9832, 2018.
30. Li Z, Jia J, Gou J, Tong A, Liu X, Zhao X and Yi T: Mmu-miR-126a-3p plays a role in murine embryo implantation by regulating Itga11. *Reprod Biomed Online* 31: 384-393, 2015.
31. Huang TC, Renuse S, Pinto S, Kumar P, Yang Y, Chaerkady R, Godsey B, Mendell JT, Halushka MK, Civin CI, *et al*: Identification of miR-145 targets through an integrated omics analysis. *Mol Biosyst* 11: 197-207, 2015.
32. Zhang HH and Li AH: Long non-coding RNA FEZF1-AS1 is up-regulated and associated with poor prognosis in patients with cervical cancer. *Eur Rev Med Pharmacol Sci* 22: 3357-3362, 2018.
33. Zhang Z, Sun L, Zhang Y, Lu G, Li Y and Wei Z: Long non-coding RNA FEZF1-AS1 promotes breast cancer stemness and tumorigenesis via targeting miR-30a/Nanog axis. *J Cell Physiol* 233: 8630-8638, 2018.
34. Zhao BS, Roundtree IA and He C: Post-transcriptional gene regulation by mRNA modifications. *Nat Rev Mol Cell Biol* 18: 31-42, 2017.
35. Dominissini D, Moshitch-Moshkovitz S, Schwartz S, Salmon-Divon M, Ungar L, Osenberg S, Cesarkas K, Jacob-Hirsch J, Amariglio N, Kupiec M, *et al*: Topology of the human and mouse m⁶A RNA methylomes revealed by m⁶A-seq. *Nature* 485: 201-206, 2012.
36. Alarcón CR, Goodarzi H, Lee H, Liu X, Tavazoie S and Tavazoie SF: HNRNPA2B1 is a mediator of m(6)A-dependent nuclear RNA processing events. *Cell* 162: 1299-1308, 2015.
37. Guo F, Li Y, Liu Y, Wang J, Li Y and Li G: Inhibition of metastasis-associated lung adenocarcinoma transcript 1 in CaSki human cervical cancer cells suppresses cell proliferation and invasion. *Acta Biochim Biophys Sin (Shanghai)* 42: 224-229, 2010.
38. Patil DP, Chen CK, Pickering BF, Chow A, Jackson C, Guttman M and Jaffrey SR: m(6)A RNA methylation promotes XIST-mediated transcriptional repression. *Nature* 537: 369-373, 2016.
39. Takada Y, Ye X and Simon S: The integrins. *Genome Biol* 8: 215, 2007.
40. Hegde S and Raghavan S: A skin-depth analysis of integrins: Role of the integrin network in health and disease. *Cell Commun Adhes* 20: 155-169, 2013.
41. Tiger CF, Fougerousse F, Grundström G, Velling T and Gullberg D: alpha1(I)beta1 integrin is a receptor for interstitial collagens involved in cell migration and collagen reorganization on mesenchymal nonmuscle cells. *Dev Biol* 237: 116-129, 2001.
42. Chai J, Modak C, Ouyang Y, Wu SY and Jamal MM: CCN1 induces beta-catenin translocation in esophageal squamous cell carcinoma through integrin alpha11. *ISRN Gastroenterol* 2012: 207235, 2012.
43. Parajuli H, Teh MT, Abrahamsen S, Christoffersen I, Neppelberg E, Lybak S, Osman T, Johannessen AC, Gullberg D, Skarstein K and Costea DE: Integrin alpha11 is overexpressed by tumour stroma of head and neck squamous cell carcinoma and correlates positively with alpha smooth muscle actin expression. *J Oral Pathol Med* 46: 267-275, 2017.
44. Reigstad I, Smeland HY, Skogstrand T, Sortland K, Schmid MC, Reed RK and Stuhr L: Stromal integrin alpha11beta1 affects RM11 prostate and 4T1 breast xenograft tumors differently. *PLoS One* 11: e0151663, 2016.
45. Zhu CQ, Popova SN, Brown ER, Barsyte-Lovejoy D, Navab R, Shih W, Li M, Lu M, Jurisica I, Penn LZ, *et al*: Integrin alpha 11 regulates IGF2 expression in fibroblasts to enhance tumorigenicity of human non-small-cell lung cancer cells. *Proc Natl Acad Sci USA* 104: 11754-11759, 2007.
46. Wu P, Wang Y, Wu Y, Jia Z, Song Y and Liang N: Expression and prognostic analyses of ITGA11, ITGB4 and ITGB8 in human non-small cell lung cancer. *PeerJ* 7: e8299, 2019.
47. Qi L, Gao C, Feng F, Zhang T, Yao Y, Wang X, Liu C, Li J, Li J and Sun C: MicroRNAs associated with lung squamous cell carcinoma: New prognostic biomarkers and therapeutic targets. *J Cell Biochem* 120: 18956-18966, 2019.

